

Generation of Entangled Photons in Graphene in a Strong Magnetic Field

Mikhail Tokman,¹ Xianghan Yao,² and Alexey Belyanin^{2,*}

¹*Institute of Applied Physics, Russian Academy of Sciences, Nizhny Novgorod 603950, Russia*

²*Department of Physics and Astronomy, Texas A&M University, College Station, Texas 77843, USA*

(Received 23 September 2012; published 14 February 2013)

Entangled photon states attract tremendous interest as the most vivid manifestation of nonlocality of quantum mechanics and also for emerging applications in quantum information. Here we propose a mechanism of generation of polarization-entangled photons, which is based on the nonlinear optical interaction (four-wave mixing) in graphene placed in a magnetic field. Unique properties of quantized electron states in a magnetized graphene and optical selection rules near the Dirac point give rise to a giant optical nonlinearity and a high rate of photon production in the mid- or far-infrared range. A similar mechanism of photon entanglement may exist in topological insulators where the surface states have a Dirac-cone dispersion and demonstrate similar properties of magneto-optical absorption.

DOI: [10.1103/PhysRevLett.110.077404](https://doi.org/10.1103/PhysRevLett.110.077404)

PACS numbers: 78.67.Wj, 42.50.Ct, 42.65.Lm

To date, the most widely used method of generating entangled photons is based on the spontaneous parametric down-conversion in a nonlinear crystal possessing a second-order nonlinearity [1,2]. In this process, a photon from a strong pump field at frequency ω_p splits into two signal photons, $\omega_p = \omega_1 + \omega_2$, which can be entangled in polarization, frequency, and wave vector. Another way to generate quantum-correlated photons through a parametric nonlinear optical process is spontaneous four-wave mixing in the optical fibers, in which two pump photons are converted into two signal photons, $2\omega_p = \omega_1 + \omega_2$, using a third-order nonlinearity of silica [3]. This process is obviously compatible with fiber communication technologies, although it does not directly lead to polarization entanglement. In both nonlinear processes the photon pair production efficiency is very low. An alternative approach using the radiative decay of biexcitons in semiconductor quantum dots [4–6] allows photon pairs to be generated on demand but requires cooling down to liquid helium temperatures.

Graphene has unusual electronic and optical properties stemming from linear, massless dispersion of electrons near the Dirac point and the chiral character of electron states [7,8]. Magneto-optical properties of graphene and thin graphite layers are particularly peculiar, showing multiple absorption peaks and unique selection rules for transitions between Landau levels [9–12]. Recent progress in growing high-quality epitaxial graphene and graphite with high room-temperature mobility and strong magneto-optical response has attracted a lot of interest and paved the way to new applications in infrared optics and photonics [13–15]. The time is ripe to explore the nonlinear and quantum optical properties of a magnetized graphene and their applications. We have recently shown that graphene placed in a magnetic field possesses perhaps the highest infrared optical nonlinearity among known materials [11]. Here we argue that an extremely strong

nonlinearity of graphene in combination with its peculiar properties of the Landau levels open new avenues for generation of the nonclassical light states, in particular polarization-entangled photons.

The proposed scheme is shown in Figs. 1 and 2. Here the energies of the Landau levels for electrons near the Dirac point are given by $\varepsilon_n = \text{sgn}(n)\hbar\omega_c\sqrt{|n|}$, where $n = 0, \pm 1, \pm 2, \dots$, $\omega_c = \sqrt{2}v_F/l_c$, $v_F \approx 10^8$ cm/s is the electron Fermi velocity, and $l_c = \sqrt{\hbar c/eB}$ is the magnetic length. We assume that the graphene is biased or doped so that the Fermi level is between the states with $n = -2$ and $n = -1$; i.e., the state $n = -2$ is occupied and the states above are empty in the absence of pumping. Two incident strong pump fields at frequencies ω_{HF} and ω_{LF} resonant to the transitions from $n = -2$ to $n = 1$ and from $n = -2$ to $n = -1$, respectively, generate two signal fields with opposite senses of the circular polarization at frequencies $\omega_{(-)}$ and $\omega_{(+)}$ that are close to resonance with transitions from $n = -1$ to 0 and from $n = 0$ to 1.

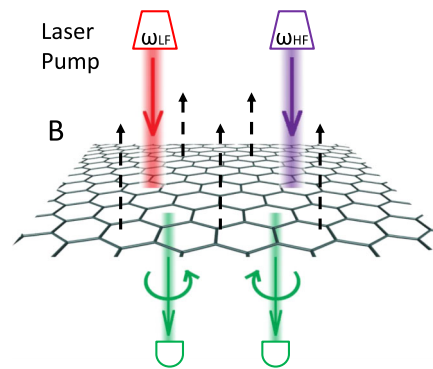


FIG. 1 (color online). Geometry of the proposed experiment. Two pump fields at frequencies ω_{HF} and ω_{LF} normally incident on a sheet of graphene placed in a magnetic field B generate entangled photons with opposite senses of the circular polarization.

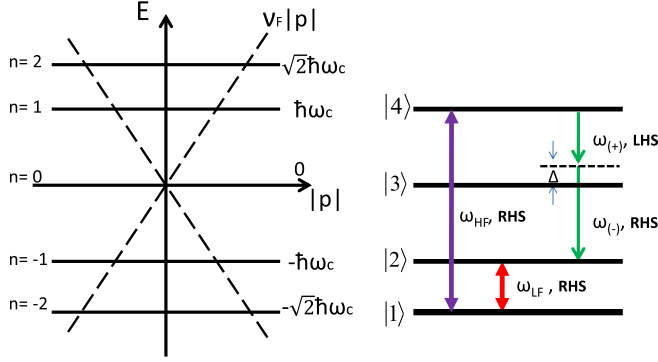


FIG. 2 (color online). Energy levels and optical transitions involved in resonant parametric generation of entangled photons in graphene. Left: Landau levels near the Dirac point superimposed on the linear electron dispersion without the magnetic field. Right: A scheme of the entangled photon generation process in the four-level system of LLs with energy quantum numbers $n = -2, -1, 0, 1$ that were renamed as states 1, 2, 3, and 4 for convenience of notation.

Note that these transitions have the same energy. Therefore, the presence of the unshifted $n = 0$ Landau level enables convenient entanglement in the polarization degree of freedom for two photons with nearly equal energies. All transition frequencies are easily tunable with a magnetic field.

The polarizations for the allowed transitions are indicated in Fig. 2. Here LHS and RHS denote left-hand and right-hand circularly polarized light with polarization vectors in the (x, y) plane of the graphene defined as $\mathbf{e}_{(\mp)} = (\mathbf{x}_0 \mp i\mathbf{y}_0)/\sqrt{2}$, respectively. Peculiar selection rules for graphene, $\Delta|n| = \pm 1$ as opposed to $\Delta n = \pm 1$ for electrons with usual parabolic dispersion, allow the transition from $n = -2$ to 1. The dipole matrix elements of the allowed transitions $d_{mn} \sim \hbar v_F / (\varepsilon_n - \varepsilon_m)$ grow fast ($\sim \lambda$) with increasing wavelength, and reach a large magnitude after introducing creation or far-infrared range; e.g., $|d_{12}|/e = 13$ nm for $B = 1$ T ($\lambda = 34$ μm). This enables an extremely high resonant third-order nonlinearity [11]. Note also that the states $n = -1, 0$, and 1 have a low population when the intensities of the optical pumps are below saturation and $\hbar\omega_c \gg k_B T$. These factors lead to a high rate of photon generation and a high signal to noise ratio.

In order to determine the optimal conditions for entanglement and the photon generation rate, we solve coupled equations for Heisenberg operators of the electron and signal photon fields, assuming that the strong pump fields are classical. Consider quasiparticles (“electrons”) on Landau levels described by stationary states $|m\rangle$ and energy levels ε_m . After introducing creation and annihilation operators of an electron, $\hat{a}_m^\dagger|0\rangle = |m\rangle$, $\hat{a}_m|n\rangle = |0\rangle$, one can define a coordinate-dependent density-matrix operator, $\hat{\rho}_{mn}(\mathbf{r}, t) = \frac{1}{\Delta V_r} \sum_j \hat{a}_{j,n}^\dagger(t) \hat{a}_{j,m}(t)$, where the index j numerates individual electrons and the summation is carried

over all electrons within a small volume ΔV_r in the vicinity of a point with radius-vector \mathbf{r} . Assuming that the operators in different points of space commute with each other, the commutation relations become

$$[\hat{\rho}_{qp}(\mathbf{r}), \hat{\rho}_{mn}(\mathbf{r}')] = \delta(\mathbf{r} - \mathbf{r}')(\hat{\rho}_{mp}(\mathbf{r})\delta_{qn} - \delta_{mp}\hat{\rho}_{qn}(\mathbf{r})). \quad (1)$$

Using the above density operator, one can write the Heisenberg operator of any physical quantity $x(\mathbf{r}, t)$ as $\hat{x} = \sum_{n,m} x_{nm} \hat{\rho}_{mn}(\mathbf{r}, t)$. In particular, the optical polarization is given by $\hat{\mathbf{P}}(\mathbf{r}, t) = \sum_{n,m} \mathbf{d}_{nm} \hat{\rho}_{mn}$.

The Heisenberg-Langevin equation for the density operator takes the form

$$\dot{\hat{\rho}}_{mn} = -\frac{i}{\hbar}(\hat{h}_{mv}\hat{\rho}_{vn} - \hat{\rho}_{mv}\hat{h}_{vn}) + \hat{R}_{mn}(\hat{\rho}_{mn}) + \hat{F}_{mn}, \quad (2)$$

independently on whether $\hat{a}_m, \hat{a}_n^\dagger$ operators obey the commutation relations for fermions or bosons.

In Eq. (2) $\hat{h}_{nm} = \varepsilon_n \delta_{nm} - \mathbf{d}_{nm} \hat{\mathbf{E}}(\mathbf{r}, t)$ is the matrix element of the Hamiltonian operator $\hat{H} = \hat{h}_{nm} \hat{a}_n^\dagger \hat{a}_m$ describing interaction with the electric field $\hat{\mathbf{E}}(\mathbf{r}, t)$ in the dipole approximation and \hat{R}_{mn} is the relaxation operator, for which we will choose the simplest form $\hat{R}_{m \neq n} = -\gamma_{mn} \hat{\rho}_{mn}$. The Langevin noise operator \hat{F}_{mn} satisfies $\hat{F}_{mn} = \hat{F}_{nm}^\dagger$ and $\langle \hat{F}_{mn} \rangle = 0$. Here the averaging $\langle \dots \rangle$ is taken both over the reservoir and over the initial state $|\Psi_E\rangle$ of the electron system. The commutators and correlators for \hat{F}_{mn} are derived in the Supplemental Material [16].

For a monochromatic electric field of a given field mode propagating in a dispersive medium with dielectric constant $\varepsilon(\omega)$, $\hat{\mathbf{E}} = \hat{\mathbf{E}}_0 e^{-i\omega t + ikz} + \hat{\mathbf{E}}_0^\dagger e^{-i\omega t + ikz}$, one can define the operators of annihilation and creation of “photons in a medium” \hat{c}_0 and \hat{c}_0^\dagger [17] as $\hat{\mathbf{E}}_0 = \mathbf{e} E_0 \hat{c}_0$, $\hat{\mathbf{E}}_0^\dagger = \mathbf{e}^* E_0 \hat{c}_0^\dagger$. Here \mathbf{e} is a unit vector of the polarization of the field and

$$E_0 = \sqrt{4\pi\hbar\omega^2 / \frac{\partial[\omega^2\varepsilon(\omega)]}{\partial\omega}}$$

is the normalization constant. With this normalization of the field operators the energy of the field in a volume V is given by $\hat{W} = \hbar\omega(V\hat{c}_0^\dagger\hat{c}_0 + \frac{1}{2})$ and their commutation relation reads $[\hat{c}_0, \hat{c}_0^\dagger] = \frac{1}{V}$. If the field amplitude varies in time and space over the scales T and L much larger than the period, $T \gg 2\pi/\omega$, and wavelength, $L \gg 2\pi/k$, one can always choose the volume of quantization $L^3 \gg V \gg (2\pi/k)^3$ and introduce space- and time-dependent creation and annihilation operators $\hat{c}_0(\mathbf{r}, t)$ and $\hat{c}_0^\dagger(\mathbf{r}, t)$ [17], which determine the photon density operator $\hat{n}_{ph} = \hat{c}_0^\dagger(\mathbf{r}, t)\hat{c}_0(\mathbf{r}, t)$.

Of course, there is no need to consider propagation of the fields through a monolayer of graphene. However, we will keep our formalism general to make it applicable to a

multilayer graphene layer which shows similar physics near the H point; see the discussion below. The 2D film limit can be retrieved from general expressions by taking the limit of an infinitely small layer thickness.

A more realistic field consists of a certain number of modes propagating within a paraxial beam of a cross-sectional area S_{\perp} . If we keep the same notation \hat{c}_0 for the field operators describing the field amplitude in the whole beam, their commutator becomes $[\hat{c}_0, \hat{c}_0^{\dagger}] = \Delta j/V$ where Δj is the number of modes. The total flux density of photons in a state $|\Psi_F\rangle$ is then given by $Q = v_{gr} S_{\perp} \langle \Psi_F | \hat{c}_0^{\dagger} \hat{c}_0 | \Psi_F \rangle$, where $v_{gr} = \frac{2c^2 k}{\partial(\omega^2 \epsilon(\omega))/\partial \omega}$ is a group velocity. It is convenient to go from a discrete set of modes to a continuous spectral interval $\Delta \omega \ll \omega$. The density of states in a volume V is equal to $\eta = V k^2 / 8\pi^3 v_{gr}$ and the wave vectors of the modes constituting a beam occupy the solid angle $\Delta \omega \approx 4\pi^2 / k^2 S_{\perp}$. One can always choose a volume V that is small on the scale of spatial variation of the operator $\hat{c}_0(\mathbf{r}, t)$, but which still includes many wavelengths of light. As a result, we arrive at the commutation relations for the operator of the field amplitude and its spectral harmonics that are specified in Eqs. (14–16) of the Supplemental Material [16].

The equation of motion for the field amplitude operator of each of the two signal fields can be derived from the Heisenberg equation for the operators of the field and electric polarization (see page 3 of the Supplemental Material [16]):

$$\left(\frac{\partial}{\partial t} + v_{gr} \frac{\partial}{\partial z} \right) \hat{c}_0 = \frac{4\pi i \omega^2}{E_0 \partial[\omega^2 \epsilon(\omega)] / \partial \omega} \hat{\mathbf{P}}_0 \mathbf{e}^*. \quad (3)$$

Equation (3) includes all the relevant effects: linear dispersion determines the group velocity of the wave, whereas the slowly varying polarization amplitude $\hat{\mathbf{P}}_0$ on the right-hand side includes nonlinearity, dissipation, and fluctuations. At the boundary z_b between the medium and the vacuum, the boundary condition for the field operator takes the form (neglecting back reflection) $\hat{c}_0(z_b)|_{\text{vacuum}} = \sqrt{\frac{v_{gr}}{c}} \hat{c}_0(z_b)|_{\text{medium}}$, which satisfies the conservation of the Poynting flux. Equation (2) is to be solved together with Eq. (3) for both signal fields in order to determine the generated signal and noise.

In the four-wave mixing process depicted in Fig. 2, the total field consists of the four waves: two strong classical pump fields at high and low frequencies resonant to the corresponding transitions between the Landau levels, $\omega_{HF} = \omega_{41}$ and $\omega_{LF} = \omega_{21}$, and two signal fields that are described by operators

$$\hat{\mathbf{E}}_{(+,-)} = \mathbf{e}_{(+,-)} E_0 \hat{c}_{(+,-)} e^{-i\omega_{(+,-)}t + ik_{(+,-)}z} + \text{H.c.} \quad (4)$$

The signal frequencies may have a detuning, $\omega_{(+,-)} = \omega_{43,32} \mp \Delta$, $\Delta \ll \omega_{+,-}$ satisfying the frequency-matching condition $\omega_{HF} = \omega_{LF} + \omega_{(+)} + \omega_{(-)}$. We also assumed that $\omega_{(+)} \approx \omega_{(-)} = \langle \omega \rangle$ in the normalization constant E_0 .

The density-matrix equations (2) for our four-level system are given in the Supplemental Material [Eq. (22)] [16]. Solving them in the steady state and in linear approximation with respect to weak signal fields, we find that optimal conditions for the entanglement are realized when the Fermi level is close to the state $|1\rangle$ ($n = -2$) and the populations of all states above are low. This is possible when the magnetic field is strong enough, $k_B T \ll \hbar \omega_c$, and Rabi frequencies of the pump fields are below saturation: $|\Omega_{HF,LF}| \ll \langle \gamma \rangle$. Here the Rabi frequencies are defined as $\Omega_{HF} = \frac{d_{14}^* E_{HF}}{\hbar}$, $\Omega_{LF} = \frac{d_{12}^* E_{LF}}{\hbar}$, and we assume for simplicity that all scattering rates γ_{mn} are of the same value $\langle \gamma \rangle$. The latter assumption can be easily dropped once the relaxation rates are known for any particular sample. If, in addition, the detuning is sufficiently large, $\langle \gamma \rangle \ll \Delta$, the only place in Eqs. (22) in the Supplemental Material [16] where we have to take into account nonzero populations of the excited states are the Langevin noise terms $\hat{F}_{(+,-)} \equiv \hat{F}_{43,32}$. Solving the density-matrix equations in the steady state and neglecting the terms of the order of $(\langle \gamma \rangle / \Delta)^2$, we arrive at the following expression for the operator of the polarization amplitude at the frequency of the signal fields:

$$\hat{\mathbf{P}}_{(+,-)} \approx \mathbf{e}_{(+,-)} (\chi \hat{E}_{(-,+)}^{\dagger} \mp id_{(+,-)} \hat{F}_{(+,-)} / \Delta), \quad (5)$$

where

$$\chi = \frac{N d_{(+)} d_{(-)}}{\hbar \Delta} \frac{(\gamma_{21} + \gamma_{41}) \Omega_{HF} \Omega_{LF}^*}{\gamma_{21} \gamma_{41} \gamma_{42}} \sim \frac{N d^2}{\hbar \Delta} \frac{\Omega_p^2}{\langle \gamma \rangle^2}, \quad (6)$$

and we denoted $\Omega_p^2 = \Omega_{HF} \Omega_{LF}^*$, $d_{(+,-)} = d_{43,32}$, $d = \hbar v_F / \omega_{32}$, and $N = \langle \Psi_E | \hat{\rho}_{11} | \Psi_E \rangle$.

Using the polarization equation (5) as a source in Eq. (3), we obtain the following coupled equations for the signal field operators:

$$\begin{aligned} \left(\frac{\partial}{\partial z} + \frac{1}{v_{gr}} \frac{\partial}{\partial t} \right) \hat{c}_{(+)} &= i\kappa \hat{c}_{(-)}^{\dagger} + \hat{G}_{(+)}, \\ \left(\frac{\partial}{\partial z} + \frac{1}{v_{gr}} \frac{\partial}{\partial t} \right) \hat{c}_{(-)}^{\dagger} &= -i\kappa^* \hat{c}_{(+)} + \hat{G}_{(-)}^{\dagger}, \end{aligned} \quad (7)$$

where the coefficient of the parametric coupling is $\kappa = 2\pi \chi \frac{\langle \omega \rangle^2}{c^2 \langle k \rangle}$ and the noise term

$$\hat{G}_{(+,-)} = \mp 2\pi i \frac{\langle \omega \rangle^2}{c^2 \langle k \rangle} \frac{d_{(+,-)} \hat{F}_{(+,-)}}{E_0 \Delta}. \quad (8)$$

Here we again neglected a small difference between the central frequencies of the signal fields in the prefactors, assuming $\omega_{(+)} = \omega_{(-)} = \langle \omega \rangle$ and $\langle k \rangle = \langle \omega \rangle / c$.

In the optimal limit of $|\Omega_p| \ll \langle \gamma \rangle \ll |\Delta|$, the noise terms and the Raman scattering of the pump fields into the signal modes can be neglected and the solution for the fields exiting a layer of thickness L takes a particularly simple and transparent form:

$$\hat{c}_{(+)}(L, t) = \cosh(\tau)\hat{c}_{(+)}(0, t - L/v_{gr}) - ie^{i\theta} \sinh(\tau)\hat{c}_{(-)}^{\dagger}(0, t - L/v_{gr}), \quad (9)$$

and similarly for $\hat{c}_{(-)}(L, t)$ after exchanging (+) and (-) subscripts. Here the parametric gain factor $\tau = |\kappa|L$ and $\kappa = |\kappa|e^{i\theta}$.

Equation (9) clearly shows the emergence of quantum correlations between the signal photons with opposite circular polarizations. In particular, consider the boundary condition at $z = 0$ corresponding to a completely uncorrelated state of vacuum fluctuations within the spectral bandwidth $\Delta\omega$. Then one can obtain from Eq. (9) that the photon fluxes in two signal fields exiting the layer at $z = L$ are completely correlated:

$$\langle 0|\hat{Q}_{(+)}(L)|0\rangle = \langle 0|\hat{Q}_{(-)}(L)|0\rangle = \frac{\Delta\omega}{2\pi} \sinh^2\tau, \\ \langle 0|(\hat{Q}_{(+)}(L) - \hat{Q}_{(-)}(L))^2|0\rangle = 0. \quad (10)$$

Here $\hat{Q}_{(+,-)}(L) = cS_{\perp}\hat{c}_{(+,-)}^{\dagger}(L)\hat{c}_{(+,-)}(L)$ are operators of the photon fluxes. The correlated (+) and (-) photons can then be used to prepare the desired polarization-entangled states. The second equation in Eqs. (10) corresponds to the Manley-Rowe relations for the parametric process. It also follows from Eq. (9) that the scheme could be used to amplify the light with a nonclassical statistics or exchange the statistical properties between (+) and (-) photons. The magnitude of $\Delta\omega$ is likely to be limited by the bandwidth of a detection system.

The Schrödinger's quantum state of entangled photons at the exit $z = L$ from the graphene layer can be calculated in the limit of small parametric gain $\tau \ll 1$ by comparing the average electric field squared calculated using Schrödinger's wave function and using our Heisenberg's solution Eq. (9); see Sec. IV A of the Supplemental Material [16]. The resulting wave function clearly describes an entangled state: $\Psi(L) = |0_{(+)}\rangle|0_{(-)}\rangle - ie^{i\theta}\tau|1_{(+)}\rangle|1_{(-)}\rangle + O(\tau^2)$. To find the terms of higher order in τ , one has to calculate the average of higher order moments of the electric field, as described in the Supplemental Material [16].

The solution Eq. (9) can be applied to predict the measurement outcome of any detection scheme sensitive to quantum correlations, for example, the heterodyne detection scheme described in Ref. [18]. As shown in Sec. IV B of the Supplemental Material [16], using Eq. (9) in calculating the average power of a heterodyned signal leads to an expression dependent on the phase difference between (+) and (-) signal photons, which is a signature of entanglement.

If noise terms \hat{G}_{+-} in Eq. (7) are taken into account, the field equations are still straightforward to solve, although the procedure becomes more cumbersome and has been moved to the Supplemental Material [16]. As a result,

the photon fluxes in Eqs. (10) acquire additional noise terms:

$$\langle 0|\hat{Q}_{(+)}(L)|0\rangle \approx \frac{\Delta\omega}{2\pi} \left(\sinh^2\tau + \frac{\gamma_{43}}{4|\kappa|\Delta} \Gamma_{(+)}(\sinh 2\tau + 2\tau) + \frac{\gamma_{32}}{4|\kappa|\Delta} \tilde{\Gamma}_{(-)}(\sinh 2\tau - 2\tau) \right),$$

and similarly for $\langle 0|\hat{Q}_{(-)}(L)|0\rangle$ after exchanging (+) and (-) subscripts. Here the factors $\Gamma_{(+,-)} = 2\pi\langle\omega\rangle^2 \times N_{4,3}|d_{(+,-)}|^2/(c^2\langle k\rangle\hbar\Delta)$ and $\tilde{\Gamma}_{(+,-)} = 2\pi\langle\omega\rangle^2 N_{3,2}|d_{(+,-)}|^2/(c^2\langle k\rangle\hbar\Delta)$ are of the order of the parametric coupling term $|\kappa|$ [see Eq. (28) in the Supplemental Material [16]]; $N_{2,3,4} = \langle\Psi_E|\hat{\rho}_{22,33,44}|\Psi_E\rangle$.

From this solution one can see that the noise contribution can be neglected if $|\Delta| \gg \langle\gamma\rangle$ provided the parametric gain is high enough: $\tau \geq 1$. For a weak amplification $\tau \ll 1$ the condition for a large signal to noise ratio is more stringent: $\Delta \gg \langle\gamma\rangle/\tau$. If this condition is not satisfied or if one of the states 2, 3, or 4 acquires a large population, then in the steady state the noise is always comparable to or greater than the signal. In this case the entangled photons can be generated only in the pulsed regime during the time of the order of a few relaxation times $1/\gamma$. This is usually the case in resonant schemes of entanglement in atomic vapors [19,20].

The above analytic results were derived in the limit of $|\Omega_p| \ll \langle\gamma\rangle \ll \Delta$. In the general case the equations can be solved numerically, including the effects of the optical pumping of electrons to excited states and optical saturation. The resulting parametric gain τ per one monolayer of graphene is plotted in Fig. 3 as a function of the frequency detuning. As seen from the figure, the magnitude of τ is around 0.01 for $\Delta \sim 10\gamma \sim 100\Omega_p$. This corresponds to a photon flux of about $10^{-4}\Delta\omega/2\pi$. To increase the value of τ for a higher rate of the twin photon generation, one can use a stack of graphene monolayers or a thin layer of graphite. Recent studies showed that a thin graphite layer maintains high carrier mobility and monolayer-like

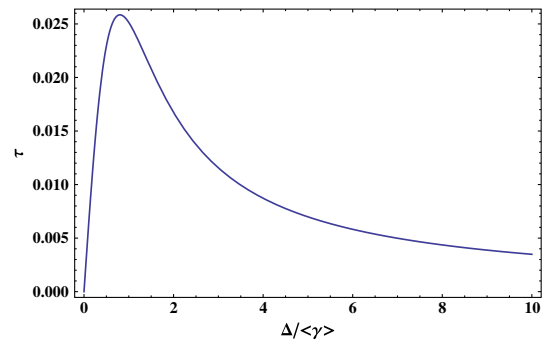


FIG. 3 (color online). Parametric gain τ per monolayer of graphene as a function of normalized detuning of the signal fields $\Delta/\langle\gamma\rangle$ for the pump field intensity $|\Omega_p|^2 = 0.1\langle\gamma\rangle^2$.

Landau levels $\propto \sqrt{|n|B}$ near the H point of the Brillouin zone [13,14], which are detectable in absorption up to 0.5 eV from the Dirac point.

Similar mechanisms of entanglement could exist in topological insulators where the surface states have a massless dispersion and demonstrate a similar pattern of Landau levels [21,22]. The band velocity v_F for surface states in $\text{Bi}_{0.91}\text{Sb}_{0.09}$ and Bi_2Se_3 inferred from measurements in Refs. [21,22] is close to that in graphene, which suggests an optical nonlinearity of similar strength. Bi_2Se_3 could be a better candidate because of its larger band gap ~ 0.3 eV and simpler single-cone band structure of the surface states. The parametric mechanism discussed in this Letter could be used to control the quantum state of electrons in surface states.

The authors are grateful to Valery Vdovin and Maria Erukhimova for helpful discussions. This work has been supported in part by NSF Grants No. OISE-0968405 and No. EEC-0540832, by the NHARP Project No. 003658-0010-2009, and by the Federal Target Program “Research and Development in Priority Directions of Development of Russia Scientific-Technological Complex” (Grant No. 07.514.11.4162).

*belyanin@tamu.edu

- [1] P. G. Kwiat, K. Mattle, H. Weinfurter, A. Zeilinger, A. V. Sergienko, and Y. Shih, *Phys. Rev. Lett.* **75**, 4337 (1995).
- [2] J. Yin, J. Ren, H. Lu, Y. Cao, H. Yong *et al.*, *Nature (London)* **488**, 185 (2012).
- [3] J. Fan, A. Migdall, and L. Wang, *Opt. Photonics News* **18**, 26 (2007).
- [4] R. M. Stevenson, R. J. Young, P. Atkinson, K. Cooper, D. A. Ritchie, and A. J. Shields, *Nature (London)* **439**, 179 (2006).
- [5] A. Mohan, M. Felici, P. Gallo, B. Dwir, A. Rudra, J. Faist, and E. Kapon, *Nat. Photonics* **4**, 302 (2010).
- [6] A. Dousse, J. Suffczynski, A. Beveratos, O. Krebs, A. Lemaitre, I. Sagnes, J. Bloch, P. Voisin, and P. Senellart, *Nature (London)* **466**, 217 (2010).
- [7] A. H. Castro Neto, F. Guinea, N. M. R. Peres, K. S. Novoselov, and A. K. Geim, *Rev. Mod. Phys.* **81**, 109 (2009).
- [8] R. R. Nair, P. Blake, A. N. Grigorenko, K. S. Novoselov, T. J. Booth, T. Stauber, N. M. R. Peres, and A. K. Geim, *Science* **320**, 1308 (2008).
- [9] M. L. Sadowski, G. Martinez, M. Potemski, C. Berger, and W. A. de Heer, *Phys. Rev. Lett.* **97**, 266405 (2006).
- [10] D. S. L. Abergel and V. I. Fal’ko, *Phys. Rev. B* **75**, 155430 (2007).
- [11] X. Yao and A. Belyanin, *Phys. Rev. Lett.* **108**, 255503 (2012).
- [12] L. G. Booshehri *et al.*, *Phys. Rev. B* **85**, 205407 (2012).
- [13] M. Orlita *et al.*, *Phys. Rev. Lett.* **101**, 267601 (2008).
- [14] M. Orlita, C. Faugeras, J. M. Schneider, G. Martinez, D. K. Maude, and M. Potemski, *Phys. Rev. Lett.* **102**, 166401 (2008).
- [15] I. Crassee, J. Levallois, A. L. Walter, M. Ostler, A. Bostwick, E. Rotenberg, T. Seyller, D. van der Marel, and A. B. Kuzmenko, *Nat. Phys.* **7**, 48 (2011).
- [16] See Supplemental Material at <http://link.aps.org/supplemental/10.1103/PhysRevLett.110.077404> for derivation of the commutators and correlators for \hat{F}_{mn} .
- [17] V. M. Fain and Ya. I. Khanin, *Quantum Electronics* (The MIT Press, Cambridge, MA, 1969), Vol. 1.
- [18] M. D. Lukin, M. Fleischhauer, A. S. Zibrov, H. G. Robinson, V. L. Velichansky, L. Hollberg, and M. O. Scully, *Phys. Rev. Lett.* **79**, 2959 (1997).
- [19] H. Xiong, M. O. Scully, and M. S. Zubairy, *Phys. Rev. Lett.* **94**, 023601 (2005).
- [20] S. Qamar, M. Al-Amri, and M. S. Zubairy, *Phys. Rev. A* **79**, 013831 (2009).
- [21] A. A. Schafgans, K. W. Post, A. A. Taskin, Y. Ando, X. L. Qi, B. C. Chapler, and D. N. Basov, *Phys. Rev. B* **85**, 195440 (2012).
- [22] P. Cheng, C. Song, T. Zhang, Y. Zhang, Y. Wang *et al.*, *Phys. Rev. Lett.* **105**, 076801 (2010).